Preliminary Studies of Cardiac Motion in Positron Emission Tomography *

Ronald H. Huesman, Gregory J. Klein,
Bryan W. Reutter, and Thomas F. Budinger
Center for Functional Imaging
E. O. Lawrence Berkeley National Laboratory
University of California

March 29, 2001

Abstract

We describe preliminary efforts to develop and implement methods for the compensation of heart motion in quantitative cardiac positron emission tomography (PET). A major hypothesis is that for the purposes of this work, the motion of the heart can be considered to be composed of two independent components: respiratory motion which changes the position and orientation of the heart, and contractile cardiac motion which changes its shape.

Over the past 20 years, the spatial resolution attainable by PET systems has improved dramatically. With this improved resolution, there is the potential to obtain detailed maps of myocardial perfusion and metabolism. However, this potential remains largely unfulfilled since current data acquisition and analysis strategies do not account for the motion of the heart, which has an amplitude more than twice the 4-5 mm resolution of contemporary commercial scanners.

Respiratory motion of the heart has been virtually ignored in cardiac emission tomography, although the problem has been recognized and was described in 1982. We and others have estimated the movement of the diaphragm and heart to be approximately 15 mm due to respiration in a human in the supine position during tidal breathing. In order to take advantage of existing and future technology in quantitative cardiac PET, methods for the compensation of heart motion must be developed.

1 Introduction

PET provides the ability to measure the moment to moment concentration of a broad variety of biologically active tracers in the organs of the body. One of its principal applications has

*This work was supported by U.S. Department of Health and Human Services grants P01-HL25840 and R01-HL50663 and by U.S. Department of Energy contract DE-AC03-76SF00098.

been in the heart, where this capability provides a unique avenue to assessing myocardial perfusion and metabolism.

Over the past 20 years, the spatial resolution attainable by PET systems has improved dramatically — a resolution of approximately 17 mm in 1974 and in the range of 4-5 mm for today's cardiac scanners. With this improved resolution, there is the potential to obtain detailed maps of myocardial perfusion and metabolism. However, this potential remains largely unfulfilled since current data acquisition and analysis strategies do not account for the motion of the heart, which has an amplitude more than twice the resolution of contemporary commercial scanners. While the resulting blurred images are reasonable qualitative estimates of the left ventricular myocardial activity, they fall far short of the high-resolution quantitative images that are potentially attainable with modern PET systems. In addition, heart motion prevents a clean separation of myocardium from blood in the ventricular cavities, thus biasing estimates of the blood pool activity and affecting the reliability of kinetic analyses used to quantify myocardial perfusion and metabolism.

Motion known as "cardiac creep" has been observed in ^{201}Tl stress-redistribution SPECT studies [1] and in ^{82}Rb rest/stress myocardial perfusion PET studies [2]. Cardiac creep is probably related to physiological changes in the volume and distribution of air in the lungs between rest and stress, which result in changes in the mean position of the diaphragm and thus the heart. An increase in mean lung volume during stress causes a downward cardiac creep, followed by a post-stress upward creep as the mean lung volume returns to normal.

The effects of gross patient motion have received much attention, particularly with respect to the misalignment that often results between transmission and emission data in PET [3, 4, 5, 6, 7, 8]. In addition, systems have been developed to help prevent patient motion during myocardial perfusion studies [9] and to monitor patient motion during radiotherapy [10].

The effects of respiratory motion of the heart have been virtually ignored in cardiac emission tomography, although the problem has been recognized and was described in 1982 [11]. We and others [12, 13] have estimated the movement of the diaphragm and heart to be approximately 15 mm due to respiration in a human in the supine position during tidal breathing. Technological development currently underway at our laboratory and elsewhere is expected to lead to better than 3 mm resolution in cardiac PET. In order to take advantage of existing and future technology in quantitative cardiac PET, methods for the compensation of heart motion must be developed.

Early work at our laboratory in gated SPECT using ^{201}Tl demonstrated feasibility as well as statistical limitations of retrospectively separating events according to the phase of the cardiac cycle [14]. We have implemented hardware for cardiac gating in the two PET scanners developed at the Lawrence Berkeley National Laboratory (the Donner 280-Crystal Positron Tomograph [15, 16, 17] and the Donner 600-Crystal Positron Tomograph [18, 19, 20]). In these devices, cardiac gating was applied prospectively. Data were separated according to time after detection of the R-wave signal from an EKG unit. PET data were routinely acquired for a sequence of time intervals within the cardiac cycle. Ungated datasets could be synthesized by summing the gated data. Lack of sufficient numbers of events often required that the data be summed in order to improve image quality for visualization. In addition, quantitative accuracy was generally not a great deal better for the gated datasets than it was for the corresponding ungated datasets. We believe now that this was due to the lack of compensation for respiratory motion of the heart in addition to the loss of events outside of a single chosen gating interval.

We expect that improvement in PET and other imaging modalities can be made if respiratory motion is removed retrospectively, obviating the need for data loss during active gating while compensating for motion artifacts. Preliminary studies to demonstrate the magnitude of cardiac wall motion and the feasibility of compensation during peak inspiration and near maximum expiration in dog (lateral) and man (supine), are described in Sections 2 and 3, respectively. Preliminary studies of the feasibility of acquiring gated data during tidal breathing in both dog and man in the supine position are described in Section 4.

2 Canine Feasibility Study

To investigate the feasibility of using gated respiratory motion compensation in cardiac PET, an anesthetized dog was injected with 23 mCi of ^{18}FDG and placed in the CTI/Siemens ECAT EXACT HR scanner. The animal was mechanically held at peak inspiration and maximum expiration positions for consecutive eight-second time periods. Separate data were acquired sequentially for the two respiratory positions, resulting in a total of 32 interleaved volume datasets for each study; half acquired during peak inspiration, half acquired during maximum expiration. These data were summed into two emission datasets and separately reconstructed. Four sets of data of this type were acquired. Ungated transmission data were acquired during normal tidal respiration and were used to correct for attenuation.

Reconstructions of the data are seen in Figure 1. The top three images show a transverse, a coronal, and a sagittal view through the 3D image volume during peak inspiration; the bottom three images show the corresponding slices acquired during expiration. An edge mask of the expiration images on top of the inspiration images shows the relative misregistration between the datasets. The data were aligned using a minimum variance of ratios technique [21] yielding a rigid-body transformation which registered the two volumes. Over the four sets of data, a 6.0 mm translation and a 6.3 degree rotation were required to align

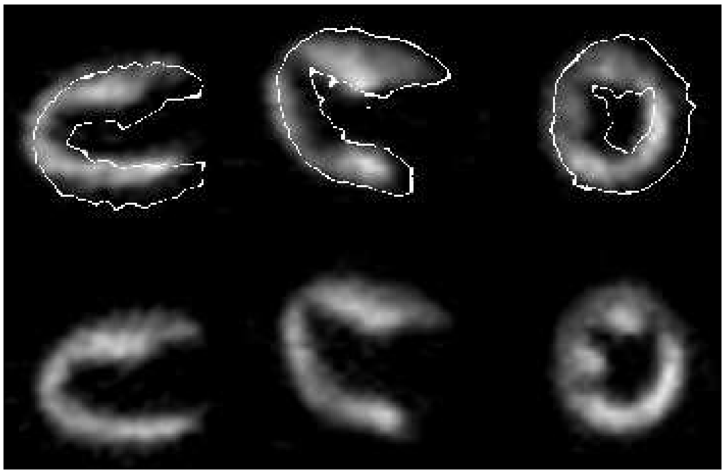

Figure 1: Transverse, coronal and sagittal views of respiratory motion between maximum inspiration (top) and expiration (bottom) in a lateral dog.

the data. Translations due to respiration in a supine human are expected to be different than those of a dog lying on its side, but they should also be repeatable, as demonstrated in the MRI study described below. Repeatable registration of the gated data allows summing of the data to improve statistics. If the images are summed without regard to misregistration, blurring occurs (Figure 2A). The blurring can be decreased by first registering the datasets

(A) 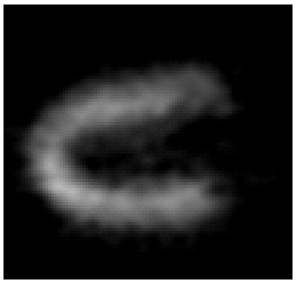 (B) 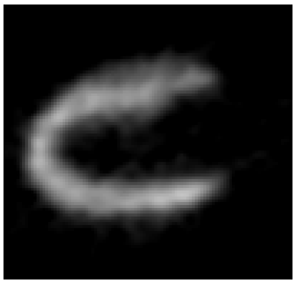

Figure 2: Summed respiratory gates (A) without registration and (B) with rigid-body registration for the dog study acquired at maximum inspiration and expiration. Considerable blurring results by summing without registration, representative of typical ungated acquisitions.

in image space, and then summing according to the transformation parameters (Figure 2B). Although the cardiac cycle was ungated in this preliminary study, it nevertheless gives evidence that substantial resolution improvement may be obtained, without loss of data, by respiratory gating and appropriately recombining the registered data.

3 Human Feasibility Study

A similar study using gated cine MRI was carried out to gauge the range of respiratory motion in the supine man. Breath-held cine MRI data were acquired using a GE Signa 1.5T scanner for two respiratory states: peak inspiration, and near maximum expiration. Each dataset consisted of 26 5-mm short axis slices and 7 cardiac gates. Figure 3A and 3B show views of the two datasets in their originally acquired orientation. Figure 3A shows the short

(A) 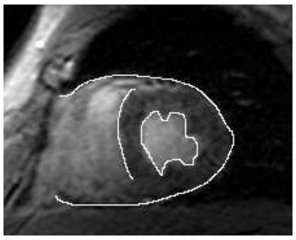 (B) 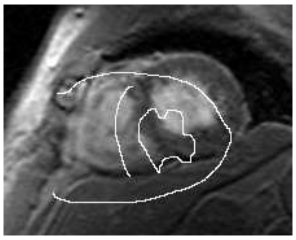 (C) 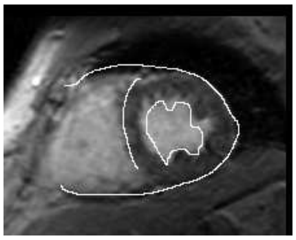

Figure 3: Cardiac Respiratory Motion in Man. (A,B) Short axis views of unregistered MR images during peak inspiration and near maximum expiration. (C) Registered view of near maximum expiration image. An edge mask of the inspiration image (A) is shown over the expiration images (B,C). A 25 mm translation is required to register the two datasets.

axis view of the first cardiac gate during peak inspiration, and Figure 3B shows the corresponding view during expiration. From the superimposed edge mask of the inspiration image on the expiration image, it is evident that considerable respiratory cardiac movement has taken place between the two states. Registration was carried out using a manual technique developed at our laboratory. Figure 3C shows the expiration datasets after having been registered to the inspiration image. For this example, a translation of 25 mm is required (13.75 mm in x, −19.06 mm in y, and 8.75 mm in z with respect to the short axis coordinate frame). The images demonstrate that a simple translation seems adequate to bring the two datasets into registration, and that the shape of the heart does not change appreciably between the two states. The extent of respiratory motion is more clearly seen using 3D surface renderings of the epicardium. Contours delineating the epicardial boundary were manually drawn on the short axis slices of each dataset and tiled together to form a triangular mesh surface model. The models are seen in Figure 4. A view of the unregistered data (Figure 4A)

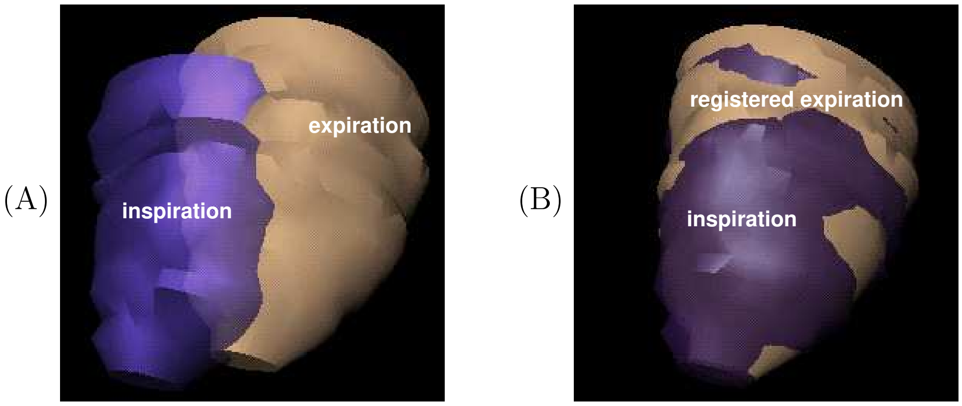

Figure 4: Extracted epicardial surfaces from peak inspiration and expiration datasets. Views of unregistered data (A) shows the considerable translation (25 mm) between the two respiratory states. View of the registered data (B) shows close agreement of the myocardial shape.

illustrates the considerable offset which would blur PET images if respiratory motion were ignored and the images were summed directly. (Phase distortions would lead to potentially worse artifacts in MRI.) However, by registering the two datasets (Figure 4B), the data could be effectively combined.

4 Hardware Gating for PET

We have modified the software and hardware of our CTI/Siemens ECAT EXACT HR tomograph to support prospective cardiac and respiratory gating. The modified tomograph front panel accepts four binary inputs which encode a desired acquisition gate. As these inputs change, tomograph events are directed to one of up to 16 different buffers in memory; each buffer representing the data from the 47 2D slices acquired for that gate.

To supply the appropriate 4-bit gating address to the scanner, we have implemented a hardware and software front end. The front end characterizes the cardiac and respiratory state of the subject being imaged from external analog cues using the LabVIEW real-time environment on a Macintosh workstation, as well as custom analog signal processing hardware. The cardiac signal is derived from standard EKG monitors. This analog EKG signal is directed to signal processing hardware which generates a pulse at each R-wave. Respiratory monitoring is achieved using a pneumatic bellows originally designed for MRI scanners (GE part no. E8811ED: Bellows Assembly for Respiratory Compensation Packages). It is secured around the patient's chest, and the analog signal from a pressure transducer connected to the bellows is amplified and input along with the R-wave pulse to a National Instruments NB-MIO-16 data acquisition board resident in the Macintosh. The Macintosh samples the signals, typically at 10 Hz for the respiratory input, and at over 600 Hz for the cardiac input. For each sample, a respiratory state is set based upon the absolute amplitude of the pressure transducer signal, and the cardiac state is set based upon the time since the last R-wave. The cardiac and respiratory states are used to select an output gating state from a 2D lookup table. This state is encoded by the National Instruments board as four binary outputs and directed to the ECAT scanner. Figure 5 summarizes the hardware and software and gives an example of one way to set up a doubly gated strategy.

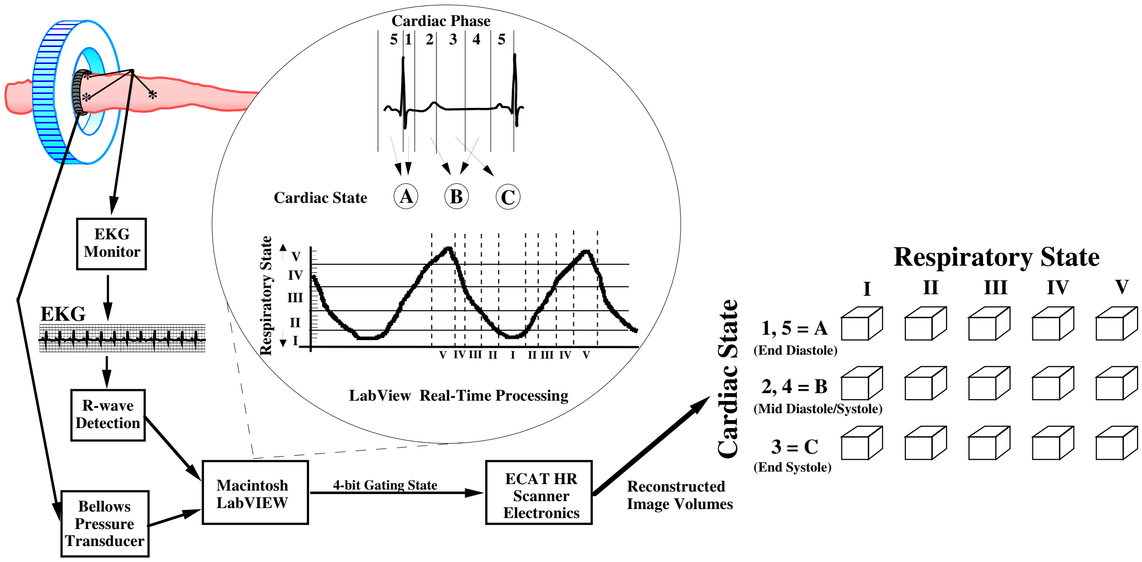

Figure 5: Schematic of doubly-gated PET acquisition. Real-time data acquisition hardware located in a Macintosh workstation processes respiratory and EKG inputs to supply the ECAT scanner with a suitable gate address. The net result of the gated acquisition is a 2D array of reconstructed image volumes.

Because of the flexibility of the LabVIEW programming environment, we have considerable latitude in choosing our ultimate method for processing the raw cardiac and respiratory inputs into a gating output state for the scanner. The LabVIEW modular programming environment allows the assembly of complex real-time switching schemes based on current and past raw inputs from a number of analog or digital inputs. Therefore, though the current scheme is quite simple, future developments using the same data acquisition board and Macintosh could include detection and adjustments for irregular heartbeats, inputs from multiple respiratory cues, or a variety of other possibilities.

4.1 Canine PET Emission Study

The current gating configuration has been used to obtain two preliminary studies indicating the feasibility of doubly-gated acquisitions. In the first, an anesthetized dog in the supine position was allowed to breath normally while an emission/transmission study was acquired using two respiratory gates and six cardiac gates. Only two respiratory gates were chosen because the anesthetized dog remained largely in the expiration state, taking only occasional, relatively shallow, quick breaths (see Figure 6A). The heart rate of the dog was approximately

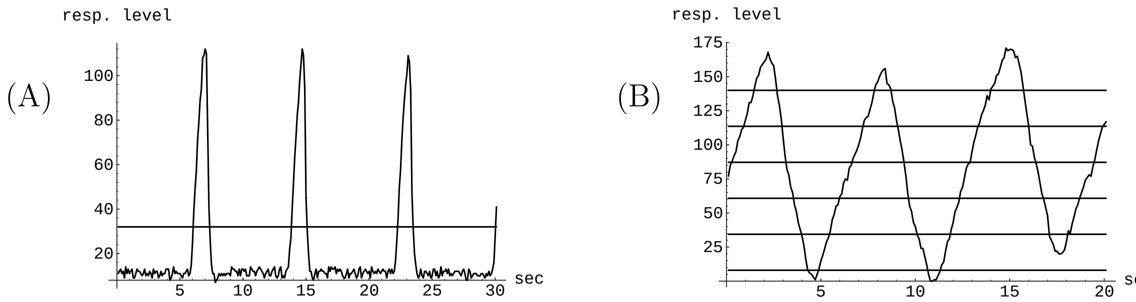

Figure 6: Bellows respiratory waveform acquired from dog (A) and human (B) studies. Horizontal lines show the thresholds used to trigger respiratory gate switching.

135 bpm, and cardiac gates were set to 60 msec intervals starting at the R-wave. A doubly-gated 60 min transmission file was first obtained to provide data for attenuation correction. The dog was then injected with 11 mCi of ^{18}FDG, which was allowed to clear from the blood pool for 30 minutes before emission imaging. Two 30-minute emission files were obtained and reconstructed. Figure 7 shows three orthogonal sections through the data for cardiac end-diastole at expiration and inspiration, and for cardiac end-systole at expiration. As was the case in the preliminary study described in Section 2, motion due to respiration is seen in Figure 7(A,B), though here, the extent of the motion is not nearly as great due to the shallowness of breathing. Shape changes due to the cardiac cycle are readily seen by comparing Figure 7(A,C). The differences seen in these gated images indicate that the hardware and software can adequately handle gate switching times typical for 60 msec cardiac gating intervals and 10 Hz respiratory sampling.

4.2 Human PET Transmission Study

To verify that the respiratory component of the gating acquisition configuration is functional, a human transmission study was carried out using respiratory gating only. In this study, the subject was fitted with the respiratory bellows around the chest and allowed to relax, breathing normally in the tomograph (Figure 6B). A 20-minute transmission scan was acquired while gating the data into 7 respiratory gates. The data from each gate were separately reconstructed, and the images were compared. Figure 8 shows orthogonal slices through the resulting image datasets from two of the gates, one acquired during the end expiration phase of the breathing cycle, the other obtained during inspiration. Comparing image sets shown in Figure 8A and Figure 8B, one can readily note the movement, especially of the diaphragm and liver. As a simple means of demonstrating the extent of motion,

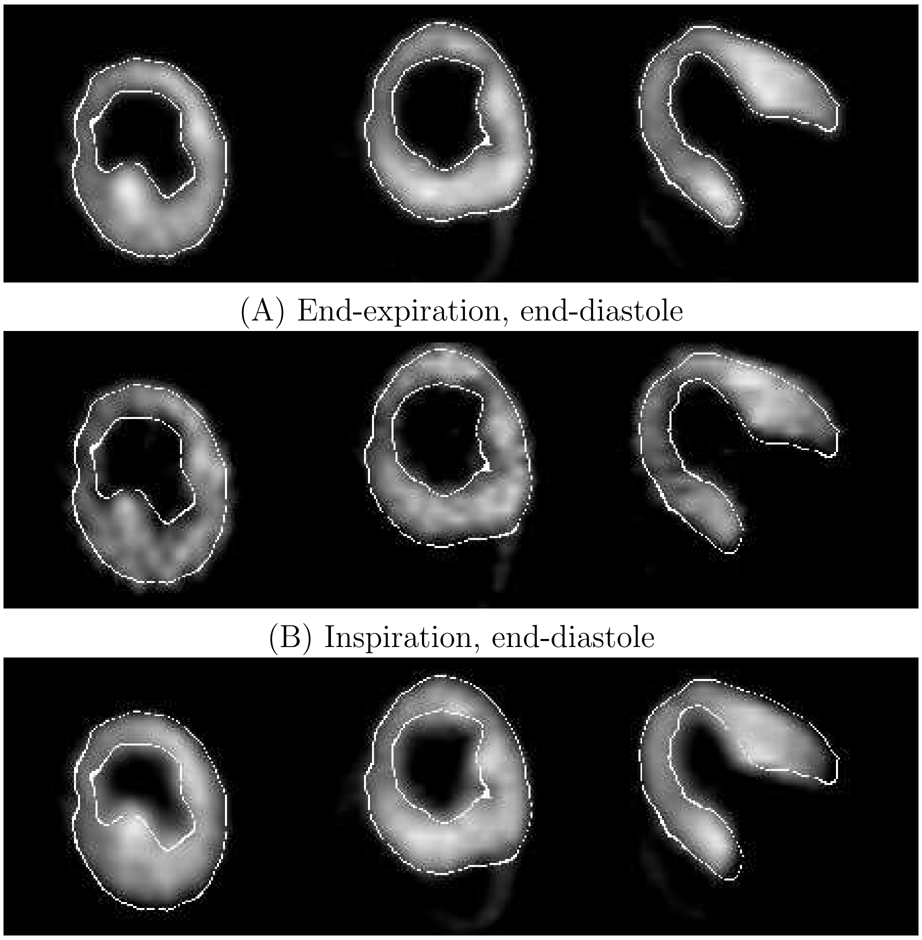

(A) End-expiration, end-diastole

(B) Inspiration, end-diastole

(C) End-expiration, end-systole

Figure 7: Three orthogonal views of doubly gated emission images of the heart in a supine dog. Because of the shallowness of breath in the anesthetized dog, heart motion due to respiration is relatively small (A,B), and little shape change is present. Heart shape changes considerably between end-diastole and end-systole (A,C). An edge mask from (A) is shown on (B,C).

Figure 8C shows the expiration dataset from Figure 8B which has been translated along the bed axis by 16 mm. A simple translation of this amount appears to bring the two respiratory gates into fairly close registration.

5 Discussion

Our basic strategy for motion correction is to acquire PET data which are gated with respect to both the cardiac and respiratory cycles. The simplest approach would be to restrict attention to a single point in the cardiac/respiratory cycle such as end-diastole/end-expiration. However, this would use only a small fraction of the acquired data, resulting in an unacceptable loss of statistical information. If both the respiratory and contractile components of

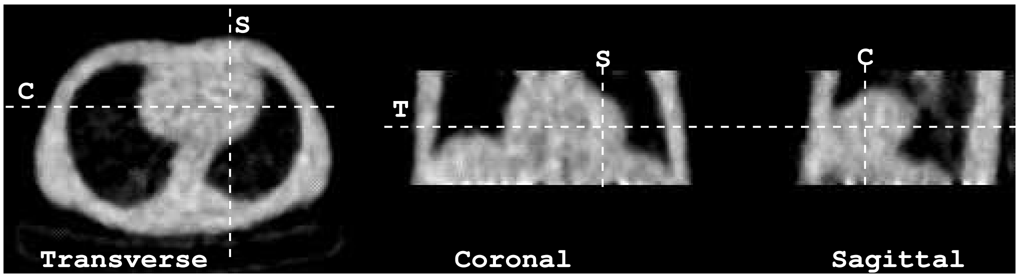

(A) End Inspiration

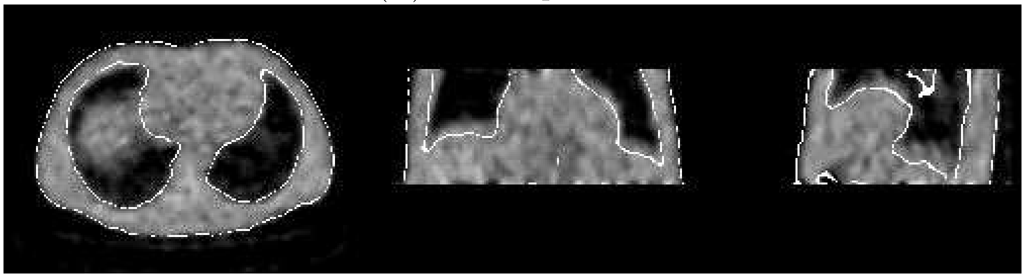

(B) End Expiration

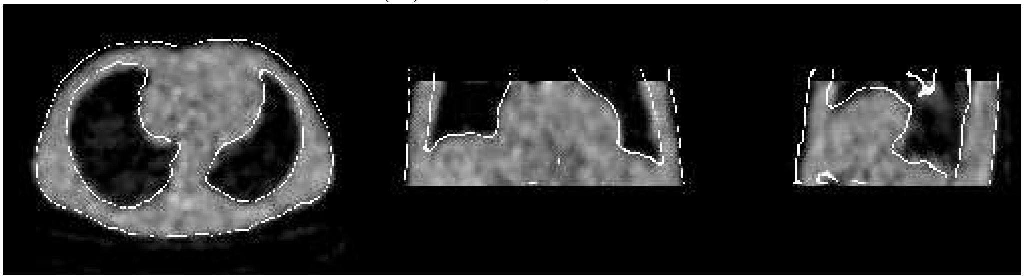

(C) End Expiration Registered to End Inspiration (Translation Only)

Figure 8: Respiratory gated human transmission study. Dotted lines are shown in (A) for reference as the intersection that each of the 3 displayed planes make with each other. A 16 mm translation is required to approximately register the end-expiration with the end-inspiration dataset (C).

heart motion are independent and can be reliably tracked from external cues, the approach can be improved by registering and summing all reconstructed volume image datasets for each cardiac gate. Registration aligns the myocardium in each respiratory gating phase to the myocardium in the end-expiration respiratory gating phase. The result will be a volume image for each phase of the cardiac contractile gating cycle in which respiratory motion artifacts have been removed from the myocardium. Stationary structures and structures that appear in an emission image which move differently than the heart, such as the liver, will be blurred in this process, but the object of this work is artifact removal from the heart at the expense of artifact generation elsewhere in the image volume.

Our approach is based on the hypothesis that the motion of the heart can be adequately modeled as the combination of two independent components: cardiac contraction and rigid-body motion (translation and rotation in space) of the heart as a whole due to respiration. Respiratory motion changes the position and orientation of the heart, and contractile motion changes its shape. While we recognize that such a model is an oversimplification due the changes in cardiopulmonary dynamics during the respiratory cycle [12, 13, 22, 23], we believe that such a model will suffice for the purposes of motion compensation artifact reduction in cardiac PET imaging. Our goal in this work is not to study the motion of the heart during respiration as such, but to compensate for the biases it introduces into the quantitative accuracy of cardiac PET data.

6 Acknowledgments

We would like to thank Dr. G.T. Gullberg for helpful discussions, Dr. K.M. Brennan, for assistance in the animal study, Dr. G.R. Caputo, for assistance in the MRI patient study, and M.H. Ho and J.H. Reed for technical assistance. This work was supported in part by the National Heart, Lung and Blood Institute of the U.S. Department of Health and Human Services under grants P01-HL25840 and R01-HL50663; and in part by the Director, Office of Energy Research, Office of Biological and Environmental Research, Medical Applications and Biophysical Research Division of the U.S. Department of Energy under contract DE-AC03-76SF00098.

References

[1] Friedman J, K Van Train, J Maddahi, A Rozanski, F Prigent, J Bietendorf, A Waxman, and DS Berman. “Upward creep” of the heart: A frequent source of false-positive reversible defects during thallium-201 stress-redistribution SPECT. *J Nucl Med*, **30**(10):1718–1722, 1989.

[2] Reutter BW, S Lim, RH Huesman, PG Coxson, GJ Klein, and TF Budinger. Cardiac creep during rest/stress myocardial perfusion studies — patient motion and lung air redistribution. *J Nucl Med*, **37**(5):131P, 1996.

[3] Huang SC, EJ Hoffman, ME Phelps, and DE Kuhl. Quantitation in positron emission computed tomography: 2. Effects of inaccurate attenuation correction. *J Comput Assist Tomogr*, **3**(6):804–814, 1979.

[4] McCord ME, SL Bacharach, RO Bonow, V Dilsizian, A Cuocolo, and N Freedman. Misalignment between PET transmission and emission scans: Its effect on myocardial imaging. *J Nucl Med*, **33**(6):1209–1214, 1992.

[5] Bettinardi V, MC Gilardi, G Lucignani, C Landoni, G Rizzo, G Striano, and F Fazio. A procedure for patient repositioning and compensation for misalignment between transmission and emission data in PET heart studies. *J Nucl Med*, **34**(1):137–142, 1993.

[6] Bacharach SL, MA Douglas, RE Carson, PJ Kalkowski, NM Freedman, P Perrone-Filardi, and RO Bonow. Three-dimensional registration of cardiac positron emission tomography attenuation scans. *J Nucl Med*, **34**(2):311–321, 1993.

[7] Yu JN, FH Fahey, BA Harkness, HD Gage, CG Eades, and JW Keyes, Jr. Evaluation of emission-transmission registration in thoracic PET. *J Nucl Med*, **35**(11):1777–1780, 1994.

[8] Andersson JLR, BE Vagnhammar, and H Schneider. Accurate attenuation correction despite movement during PET imaging. *J Nucl Med*, **36**(4):670–678, 1995.

[9] Cooper JA and BK McCandless. Preventing patient motion during tomographic myocardial perfusion imaging. *J Nucl Med*, **36**(10):2001–2005, 1995.

[10] Gerig LH, SF El-Hakim, J Szanto, D Salhani, and A Girard. The development and clinical application of a patient position monitoring system. *Proc SPIE*, **2350**:59–72, 1994.

[11] Ter-Pogossian MM, SR Bergmann, and BE Sobel. Influence of cardiac and respiratory motion on tomographic reconstructions of the heart: Implications for quantitative nuclear cardiology. *J Comput Assist Tomogr*, **6**(6):1148–1155, 1982.

[12] Fredrickson JO, H Wegmüller, RJ Herfkens, and NJ Pelc. Simultaneous temporal resolution of cardiac and respiratory motion in MR imaging. *Radiology*, **195**:169–175, 1995.

[13] Wang Y, SJ Riederer, and RL Ehman. Respiratory motion of the heart: Kinematics and the implications for the spatial resolution in coronary imaging. *Magn Reson Med*, **33**(5):713–719, 1995.

[14] Budinger TF, JL Cahoon, SE Derenzo, GT Gullberg, BR Moyer, and Y Yano. Three dimensional imaging of the myocardium with radionuclides. *Radiology*, **125**(2):433–439, 1977.

[15] Derenzo SE, PG Banchero, JL Cahoon, RH Huesman, T Vuletich, and TF Budinger. Design and construction of the Donner 280-crystal positron ring for dynamic transverse section emission imaging. In *Proceedings of the 1977 IEEE Conference on Decision and Control*, volume 1, pages 341–349, 1977. IEEE 77CH1269-OCS.

[16] Derenzo SE, TF Budinger, JL Cahoon, WL Greenberg, RH Huesman, and T Vuletich. The Donner 280-crystal high resolution positron tomograph. *IEEE Trans Nucl Sci*, **NS-26**(2):2790–2793, 1979.

[17] Huesman RH and JL Cahoon. Data acquisition, reconstruction and display for the Donner 280-crystal positron tomograph. *IEEE Trans Nucl Sci*, **NS-27**(1):474–478, 1980.

[18] Derenzo SE, RH Huesman, JL Cahoon, A Geyer, D Uber, T Vuletich, and TF Budinger. Initial results from the Donner 600 crystal positron tomograph. *IEEE Trans Nucl Sci*, **NS-34**(1):321–325, 1987.

[19] Cahoon JL, RH Huesman, SE Derenzo, AB Geyer, DC Uber, BT Turko, and TF Budinger. The electronics for the Donner 600-crystal positron tomograph. *IEEE Trans Nucl Sci*, **NS-33**(1):570–574, 1986.

[20] Derenzo SE, RH Huesman, JL Cahoon, AB Geyer, WW Moses, DC Uber, T Vuletich, and TF Budinger. A positron tomograph with 600 BGO crystals and 2.6 mm resolution. *IEEE Trans Nucl Sci*, **NS-35**(1):659–664, 1988.

[21] Woods RP, JC Mazziota, and SR Cherry. Rapid automated algorithm for aligning and reslicing PET images. *J Comput Assist Tomogr*, **16**(4):620–633, 1992.

[22] Hoffman EA and EL Ritman. Heart-lung interaction: Effect on regional lung air content and total heart volume. *Ann Biomed Eng*, **15**(3):241–257, 1987.

[23] Hoffman EA. Interactions: The integrated functioning of heart and lungs. In Sideman S and R Beyer, editors, *Interactive Phenomena in the Cardiac System*, chapter 34, pages 347–364. Plenum Press, New York, 1993.